CHAPTER II

THEORETICAL BACKGROUND AND LITERATURE REVIEW

2.1 Background

In the present, hydrogen is considered an energetic vector able to play a role of increasing importance in future energy system, concerning in particular clean production (Basile *et al.*, 2005). In additon, hydrogen can be produced from renewable
sources such as biomass, solar energy, and so on, and is efficiently converted to electricity by PEM fuel cells (Faungnawakij *et al.*, 2006). According to PEM fuel cells, hydrogen is considered as an attracttive to the conventional gasoline internal combustion, and required storage infrastructure either in high pressure or generated on-board using a liquid hydrogen (Patel *et al.*, 2007). The PEM fuel cells have presently attracted much attention worldwide since it provides high efficiency with clean exhaust gas by consuming hydrogen and oxygen (Faungnawakij *et al.*, 2006). This system offers higher potential for efficiency and reduces emission of pollutants in power generation when compare with burning fossil fuel (Chang *et al.*, 2007). In order to the growing attention on the fossil fuel crisis and environment pollution imposed consider new and clean processes and renewable materials for generation as using hydorgen by PEM fuel cells (Iulianeli *et al.*, 2009) that can be replace the fossil-based energy in the future. Thus the hydorgen production must be evaluated for the suitable process and condition.

2.2 Hydrogen Production from Methanol (CH_3OH)

Presently, direct storage and use of hydrogen on PEM fuel cell vehicle have certain limitations; therefore, on-board hydrogen production from hydrocarbon fuels such as methanol, ethanol, dimethyl ether, and etc. are being considered as a potential option (Patel *et al.*,2007). Among all the contenders, the methanol has been recommended as the best source for hydrogen fuel-cell engines in transportation

applications because of the high energy density liquid fuels, due to the high H/C ratio having a lower propensity for soot formation than other hydrocarbons, relatively low boiling point and easy storing. In addition, its safe handling, low cost, and ease of synthesis from a variety of feedstocks (biomass, coal, and natural gas) (Shishido *et al.*, 2007). Moreover, using methanol to produce hydrogen no carbon-carbon bond (minimizing coke formation), no sulfer presents in the fuel, and current infrastructure of gasoline can be used for storage (Patel *et al.*, 2007).

Methanol can be prepared particularly from synthesis gas (syn-gas, a mixture of CO_2 and H_2) obtained from the incomplete combustion of fossil fules (generally natural gas or coal), and production of methanol is also possible by the oxidative conversion of methane, avoiding the initial preparation of syn-gas, or by reductive hydrogenative conversion of CO_2 (from industrial exhausts of fossil fuel burning power plants, cement plants, etc. and eventually the atmosphere itself). Methanol can also be converted from agricultural wastes (biomass) as an alternative way to manage agricultural waste. Moreover, methanol can already be used as substitutes for gasoline and diesel fuel in today's internal combustion engine-powered cars and it can convert to hydrogen which is the most common base material in the universe. Technology for converting methanol into a hydrogen-rich stream is mainly based on steam refoming of methanol (SRM), partial oxidation of methanol (POM), and combination of both as oxidative steam reforming of methanol (OSRM).

2.2.1 Steam Reforming of Methanol (SRM)

The steam reforming reaction is viewed as a very interesting and promising method for hydrogen production useful for fuel cell applications. The chemical reactions considered for describing the SRM process are the following:

$$CH_3OH + H_2O \leftrightarrow CO_2 + 3H_2, \quad \Delta H°_{298K} = +49.7 \text{ (kJ/mol)} \tag{2.1}$$

$$CO + H_2O \leftrightarrow CO_2 + H_2, \quad \Delta H°_{298K} = -41.2 \text{ (kJ/mol)} \tag{2.2}$$

$$CH_3OH \leftrightarrow CO + 2H_2, \quad \Delta H°_{298K} = +90.7 \text{ (kJ/mol)} \tag{2.3}$$

The overall reaction for SRM, as equation 2.1, and the decomposition of methanol (DCM) as equation 2.3. These are endothermic and proceed under volume increase, while the water gas shift (WGS) reaction (Equation 2.2) is exothermic and proceeds without volume change (Iulianelli *et al.*, 2008). Actually, steam reforming is the most used technology for producing hydrogen that more suitable for stationary applications owing to a slow start-up. It is favorable at high temperature (250–350 °C), and low pressure (Armor *et al.*, 2008). However, it is an endothermic process, needing heat to be supplied (Iulianeli *et al.*, 2009).

The steam reforming process is usually operated with excess steam, to induce the WGS reaction in the reformer in order to lower the CO concentration in the product gas. The main drawback of SRM is the selectivity to CO as a by-product, an issue particular important when produce hydrogen for fuel cell applications, the reformed hydrogen-rich stream needs purification before being fed to PEM fuel cell. The purification of a reformed stream is a crucial aspect and is mainly devoted to remove the CO, responsible with a content >10 ppm of the anodic catalyst poisoning of a PEM fuel cell. (Bichon *et al.*, 2006).

Not only CO is usually found in the product stream but also methane, depending upon the type of catalyst, and the operating conditions. The formation of methane consumes hydrogen production from methanol and steam, resulting as suppressing the production of hydrogen gas that shown in Equation 2.4.

$$CO(g) + H_2(g) \rightarrow CH_4(g) + H_2O(g) \qquad \Delta H^\circ_{298K} = -206\ kJmol^{-1} \tag{2.4}$$

Both CO formation and CH_4 formation in SRM reaction can be produced carbon formation. H_2 production operation concerns with regard to carbon formation. Carbon formation can build rapidly and shut down the process, thus it is important to keep it under control. There are two major pathways for carbon formation:

$$2CO \rightarrow CO_2 + C \tag{2.5}$$

$$CH_4 \rightarrow C + 2H_2 \tag{2.6}$$

The SRM can also lead to the formation of toxic and undesirable products such as formic acid (HCOOH), formaldehyde (CH_2O), and dimethylether (CH_3OCH_3), which limit the hydrogen (Houteit *et al.*, 2006).

The simplified process flow diagram for SRM is shown in Figure 2.1, illustring the major unit operations.

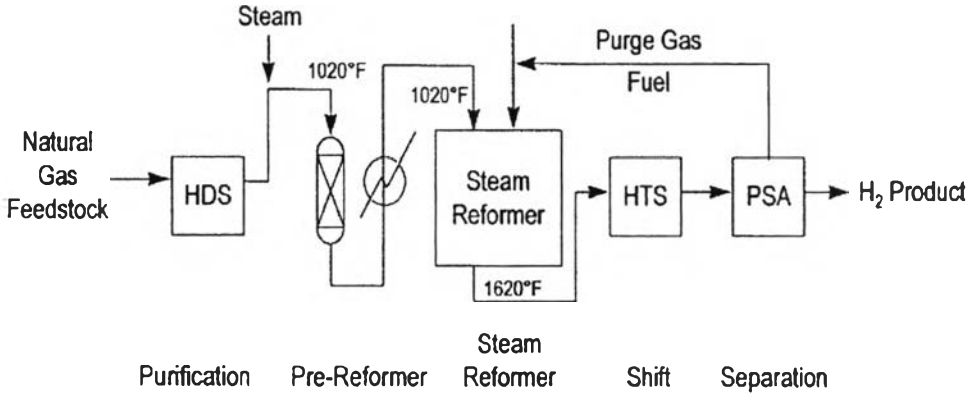

Figure 2.1 Simplified process flow diagram for SRM (Armor *et al.*, 2008).

Many researchers still keep going on searching the improvement of SRM process by using experimental conditions, and catalysts to produce higher hydrogen production that avoid the risk of coke formation, high content of CO, and other by-products. Particularly CO clean-up step of hydrogen prior to the fuel cells have been focused.

2.2.1.1 Experimental Condition

The effect of reaction temperature on the catalytic performance is shown in Figure 2.2. The methanol conversion increased with increasing the reaction temperature, while methanol is converted almost completely into H_2, CO_2 and CO up to 280°C.

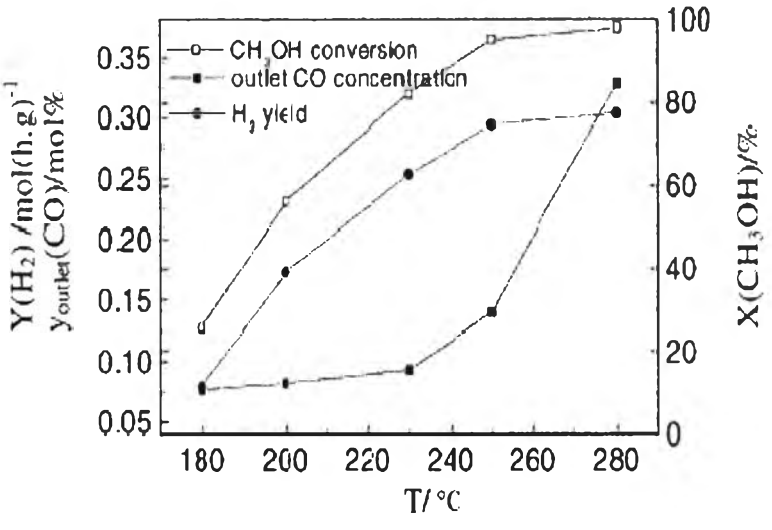

Figure 2.2 Effect of reaction temperature in methanol steam reforming reaction (Zhang *et al.*, 2003).

The reaction temperature is also effect on the formation rate is shown in figure 2.3. The profiles of H_2, CO_2, and CO formation rates went up to the maximum and then decreased with time; the extents of both going up and coming down of the rates increase with increasing reaction temperature. The formation rate of CO is very small at these reaction temperatures.

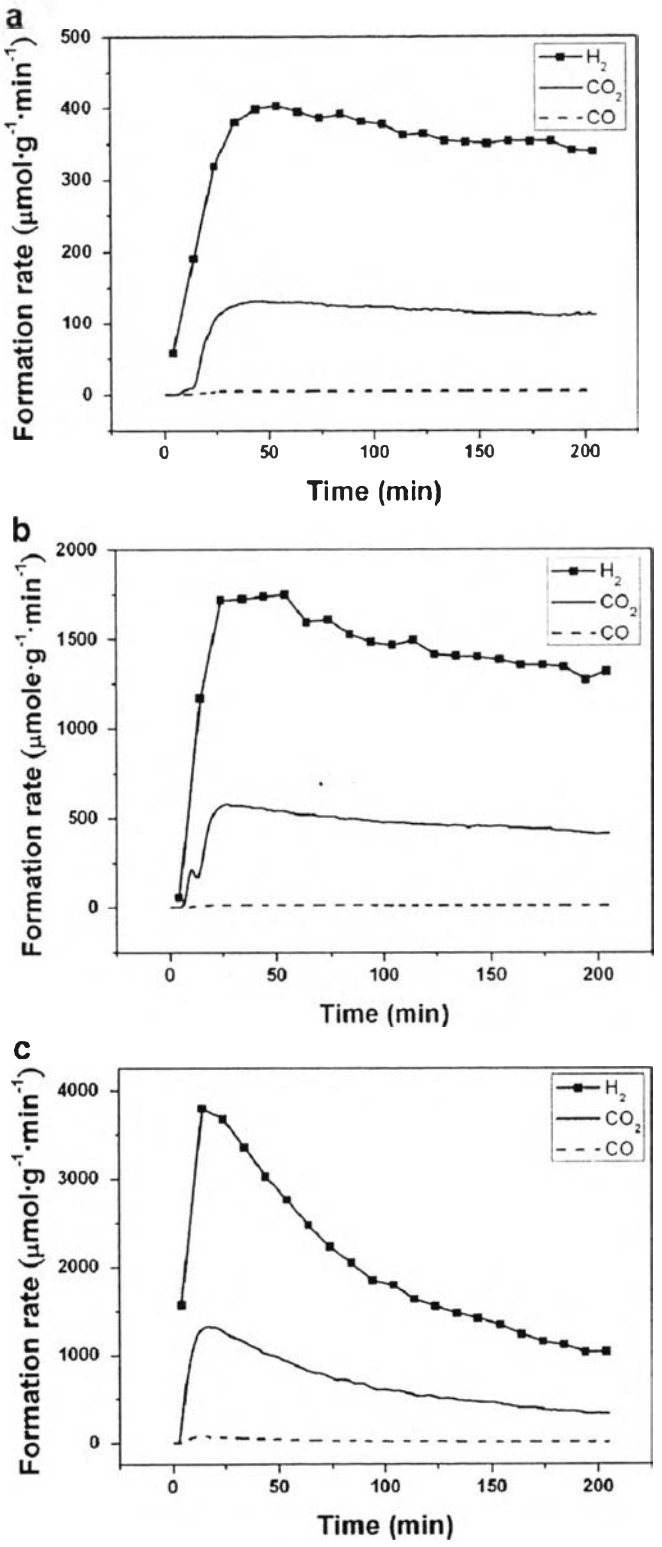

Figure 2.3 Effect of reaction temperature on product profiles with 0.1 g of 5% Cu/GDC, (a) 210 °C, (b) 240 °C, and (c) 270 °C (Huang *et al.*, 2010).

The effect of the steam:methanol ratio on the catalytic activity was also investigated. Figure 2.4 shows a comparison of the CO concentration at two steam:methanol ratios. The $CuO–ZnO–Al_2O_3$ catalysts are a considerable decrease in the CO concentration at high conversions when the steam ratio is slightly increased. It has been noted earlier that an excess of steam aids in inhibiting CO formation.

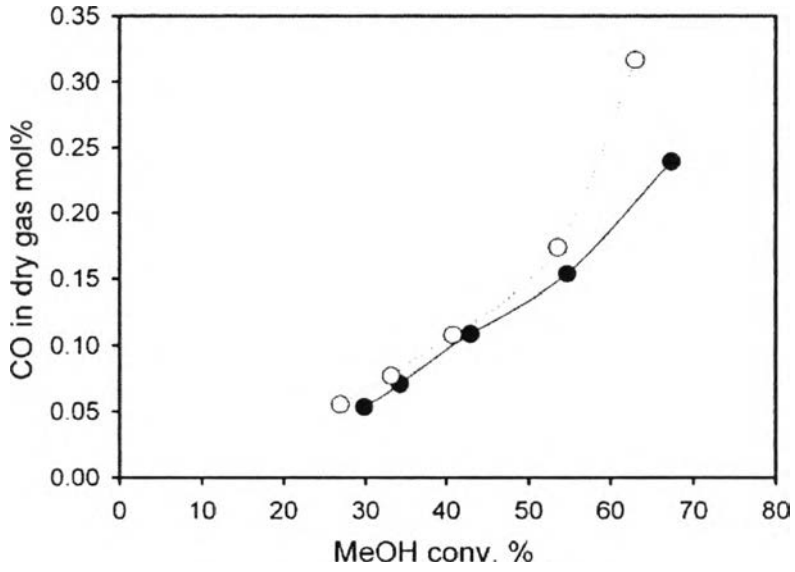

Figure 2.4 The influence of the steam:methanol ratio on CO production. Open symbols: H_2O:MeOH = 1.3, filled symbols: H_2O:MeOH = 1.1. LHSV = 11.2 h^{-1}, T = 473.523 K (Bichon *et al.*, 2006).

2.2.1.2 Mechanism and Kinetics of Methanol Steam Reforming

There are limited kinetic studies and reaction mechanisms data available for the SRM process. The individual reactions (Equations 2.1–2.3) to be included in the kinetic model of the SRM process are still under debate. Initially, SRM was supposed to proceed by the formation of CO and H_2 (DCM), followed by the WGS reaction. The formation of CO_2 by the direct reaction of methanol and steam has also been proposed (Mastalir *et al.*, 2005). Therefore, its concentration in the product stream must be equal to or greater than the concentration of CO at the WGSR equilibrium. The elementary surface reaction mechanisms and derived the

Langmuir–Hinshelwood expression. They suggested that CO was formed via decomposition of methyl formate (Equations 2.7–2.9).

$$2CH_3OH \rightarrow CH_3OCHO + 2H_2 \quad (2.7)$$

$$CH_3OCHO + H_2O \rightarrow HCOOH + CH_3OH \quad (2.8)$$

$$HCOOH \rightarrow CO_2 + H_2 \quad (2.9)$$

The kinetic expression from this predicts the rates of methanol conversion and carbon dioxide formation. They neglect the CO formation that cannot be neglected as even very low CO concentration can poison the Pt anode of PEM fuel cell. Peppley *et al.* (1999) developed a LH rate expression considering SRM, DCM, and WGS reactions with dual site mechanism. It can be seen that in all the reaction mechanisms the route of CO formation is different. The study CO formation mechanism through DRIFT analysis and confirmed that the CO formation over $CuO/ZnO/ZrO_2/Al_2O_3$ catalyst for SRM occurs via (RWGS) reaction (Equation 2.10). After that, many researchers have also proposed the CO formation via RWGS (Agrell *et al.*, 2001; Reuse *et al.*, 2004) that uses the products of the reforming reaction i.e. H_2 and CO_2.

$$CO + H_2O \leftrightarrow CO_2 + H_2, \qquad \Delta H^\circ_{298\,K} = -41\ kJmol^{-1} \quad (2.10)$$

The kinetic study of steam reforming of methanol was carried out over $Cu/ZnO/Al_2O_3$ catalyst with composition $Cu/ZnO/Al_2O_3$:10/5/85 (wt%). The concentration of CO in the product gas was less than 1% and was always well below the equilibrium CO concentration of the WGS. This supports the reaction sequence of methanol steam reforming followed by the RWGS (Patel *et al., 2007*).

Based on the extensive testing of the $CuO/ZnO/Al_2O_3$, a semi-empirical model of the kinetics of the SRM has been developed by using the reaction schemes of irreversible reaction of SRM and DCM reaction. They found that the WGS could be neglected without substantial loss in accuracy. The rate equations for both reactions can be written as follows:

$$r_{CH3OH} = -k_1 C_{CH3OH} - k_2$$
$$r_{H2O} = -k_1 C_{CH3OH}$$
$$r_{CO2} = k_1 C_{CH3OH}$$
$$r_{CO} = k_2$$
$$r_{H2} = 3k_1 C_{CH3OH} + 2k_2$$

Given the rate constants k_1 and k_2, it is fairly simple to numerically integrate this system of equations for an isothermal bed to obtain the predicted performance of the reformer.

The reaction rate of methanol and water consumption is depending only on the concentration of methanol but no depending on water concentration. Furthermore, the reaction rate of CO formation is a zero-order rate, which means that the formation of CO is not affected by the concentration of methanol or the concentration of water (Amphlett *et al.*, 1994)

2.2.2 Partial Oxidation of Methanol (POM)

Partial oxidation of methanol is an attractive on-site source of H_2 for fuel cells. This is an exothermic reaction according to equation:

$$CH_3OH(g) + 1/2O_2(g) \rightarrow 2H_2(g) + CO_2(g), \ \Delta H°_{298K} = -192 \text{ kJmol}^{-1} \quad (2.11)$$

However, a number of other reactions can take place at the same time. These are mainly methanol total oxidation (Equation 2.12), methanol decomposition (Equation 2.13), steam reforming (Equation 2.14), water-gas shift (Equation 2.15), methanation (Equation 2.16), and CO (Equation 2.17) and H_2 (Equation 2.18) oxidation:(Pe´rez *et al.*, 2007)

$$CH_3OH + 3/2O_2 \leftrightarrow CO_2 + 2H_2O \quad (2.12)$$
$$CH_3OH \leftrightarrow CO + 2H_2 \quad (2.13)$$
$$CH_3OH + H_2O \leftrightarrow 3H_2 + CO_2 \quad (2.14)$$
$$CO + H_2O \leftrightarrow CO_2 + H_2 \quad (2.15)$$
$$CO + 3H_2 \leftrightarrow CH_4 + H_2O \quad (2.16)$$

$$CO + 1/2O_2 \leftrightarrow CO_2 \quad (2.17)$$

$$H_2 + 1/2O_2 \leftrightarrow H_2O \quad (2.18)$$

The POM reaction to produce H_2 has many advantages exist over the SRM since using oxygen (or air) instead of steam as the oxidant offers an exothermic reaction, more favorable thermodynamically, that resulting in more energy efficient. It can lessen the time needed for the apparatus to reach the working temperature from cold start-up and work under thermo-balanced conditions. In addition, it has been reported that the reaction rate of partial oxidation over copper catalysts is higher than the steam reforming reaction. However, the POM process is highly exothermic, heat must be removed from the reactor, and it could be difficult to control the temperature of the system (Wang *et al.*, 2003).

2.2.2.1 Catalytic Activity

The copper-zinc catalysts are very active for the POM to produce hydrogen and a typical reaction profile is shown in Figure 2.5. This process operates in low temperature range. It can be observed that at 215 °C the reaction sets on and the rates of methanol and oxygen conversion strongly increase with the temperature to produce selectively H_2 and CO_2. The rate of CO production is very low throughout the temperature range from 200 to 225 °C, the H_2O formation decreases at temperatures higher than 215 °C and no other products were observed.

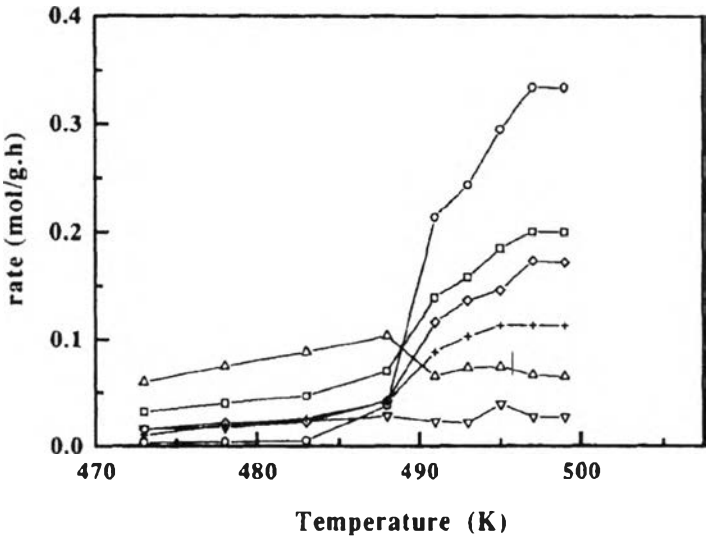

Figure 2.5 Partial oxidation of methanol over the catalyst $Cu_{40}Zn_{60}$: (□), CH3OH conversion; (+), O_2 conversion; (○), H_2; (◊), CO_2; (Δ), H_2O;(∇), CO (Alejo *et al.*, 1997).

The effect of copper content on methanol conversion, H_2, and CO_2, is shown in Figure 2.6. Methanol conversion to H_2 and CO_2 increases with the copper content reaching a maximum with the catalyst $Cu_{40}Zn_{60}$ and decreasing for higher copper loadings. A relationship between the POM and the copper metal surface area can also be clearly observed. The catalyst $Cu_{40}Zn_{60}$, which has the highest copper metallic area, is the most active and selective for the POM.

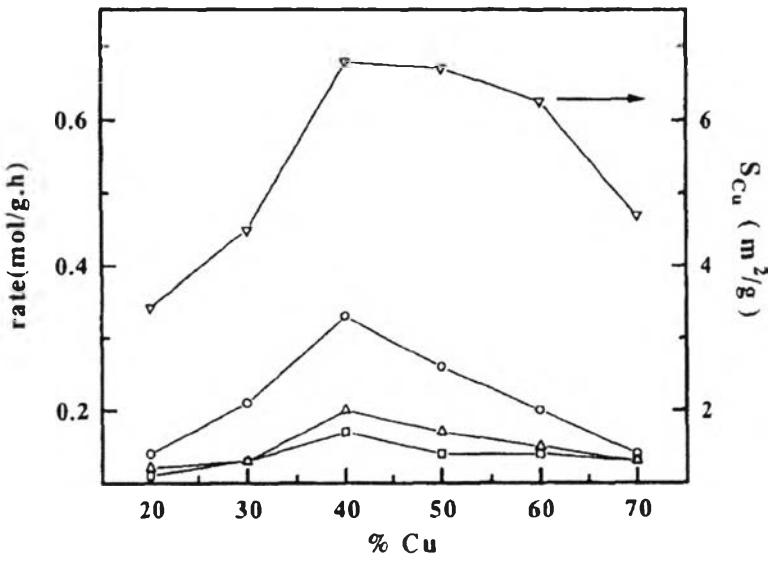

Figure 2.6 Rates of methanol conversion (Δ) and H_2 (○) and CO_2 (□) formation at 497 K and copper metallic area (∇) versus the copper content in the Cu-Zn catalysts (Alejo *et al.*, 1997).

2.2.2.2 Experimental Condition

The effect of O_2/CH_3OH molar ratio on the activity of Au–Ru/Fe_2O_3 catalysts for POM at 250 °C is illustrated in Figure 2.7. The result showed that an increase in O_2/CH_3OH molar ratio from 0.1 to 0.6, the amount of oxygen increases, methanol conversion increases from 52.0 to 100%. On the other hand, the hydrogen selectivity decreases with consequent increase in the selectivity of water. This could be due to fast oxidation of hydrogen formed in the reaction (Equation 2.18). For CO selectivity was decreased with an increase in O_2/CH_3OH molar ratio due to the more availability of oxygen. Since a O_2/CH_3OH molar ratio of 0.5 showed higher hydrogen selectivity with complete conversion of methanol.

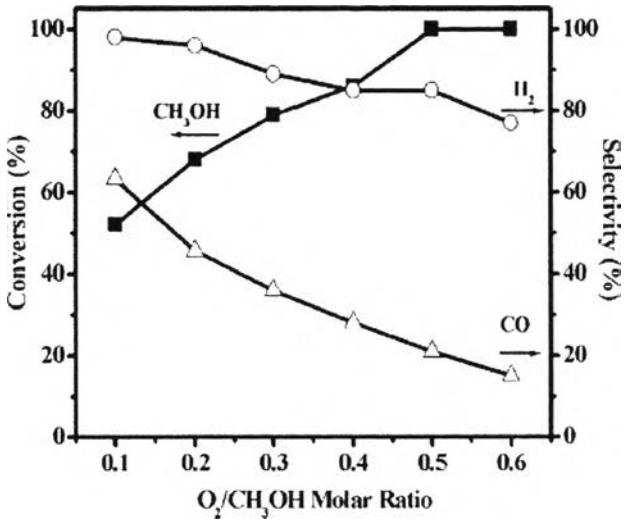

Figure 2.7 Effect of O_2/CH_3OH molar ratio on methanol conversion, hydrogen selectivity and CO selectivity for POM over Au–Ru/Fe_2O_3 catalysts (calcination temperature, 673 °C; reaction temperature, 523 °C; reaction time, 10 min) (Chang *et al.*, 1997).

2.2.3 Oxidative Steam Reforming of Methanol (OSRM)

The OSRM or autothermal reforming of methanaol (ATRM), the simultaneous partial oxidation and steam reforming processes, can be a promising way due to its energy saving, fast startup, and quick response of the overall reaction. This reaction is also referred as auto-thermal reforming, when operated under adiabatic conditions. The equation can be written as:

$$CH_3OH_{(g)} + (1\text{-}p)H_2O_{(g)} + 0.5pO_{2(g)} \rightarrow (3\text{-}p)H_{2(g)} + CO_{2(g)},$$
$$\Delta H°_{298K} = -241.8p + 49.5\ kJmol^{-1} \qquad (2.18)$$

The overall heat of reaction depends upon the value of p, which directly influences the thermal properties of the OSRM system as well as hydrogen concentration (Patel *et al.*, 2007).

Compared with SRM, the OSRM reaction has the advantages of a smaller reactor volume, a simpler reactor design (Turco *et al.*, 2007), and the reaction to proceed much higher rates in the reactor (Perez *et al.*, 2007). In addition, the OSRM reaction combines the advantages of SRM in terms of higher hydrogen yield

and lower CO formation and those of POM in terms of more rapid response to changes in the power demand and a faster cold start-up in engine. The OSRM reaction could be from endothermic to exothermic when the oxygen/methanol ratio in the feed increases. Hence it could offer an effective way to regulate the reaction temperature in the reactor and less heat exchange between cold and hot streams is required. This makes the reformer compacter especially important for transportation fuel cell applications (Hong *et al.*, 2008). Unfortunately, the OSRM process produces CO as a by-product in appreciable amounts which causes the poison for the Pt anodes of PEM fuel cells, and also suppresses the hydrogen's purity. To improve the activity of this reaction, the catalysts must be required in terms of high methanol conversion, high hydrogen selectivity, generating by the same time with minimizing of CO formation.

2.2.3.1 Experimental Condition

The effect of the temperature on the gas effluent composition in SRM and OSRM reactions over $Zn_{10}Ti_{90}$ is shown in Figure 2.8. For both reactions, the main products are H_2 and CO_2. The activity of the catalyst is negligible below 300 °C and above this temperature, it is active in methanol reforming (increasing of H_2, CO_2, and decreasing of CH_3OH and H_2O (and O_2 in OSRM)). The reactions are strongly influenced by the temperature and are complete at 400 °C. In both processes, CO and dimethylether ($(CH3)_2O$) are formed as by-products according to Equation 2.19. Methane is also produced in the SRM process. At a higher temperature than 350 °C $(CH_3)_2O$ can react over titania surface in the presence of hydrogen, forming methane and water according to Equation 2.20. Thus, at temperature greater than 350 °C, $(CH_3)_2O$ starts decreasing and simultaneously methane starts increasing in the SRM process.

$$2CH_3OH \rightarrow (CH_3)_2O + H_2O \quad (2.19)$$

$$(CH_3)_2O + 2H_2 \rightarrow 2CH_4 + H_2O \quad (2.20)$$

In the OSRM reaction, no methane is detected probably because the presence of O_2 suppresses CH_4 formation is shown in Equation 2.21.

$$CH_4 + O_2 \rightarrow CO_2 + 2H_2 \qquad (2.21)$$

In the OSRM process, the CO content is lower than in the SRM process, probably because of it oxidation to CO_2.

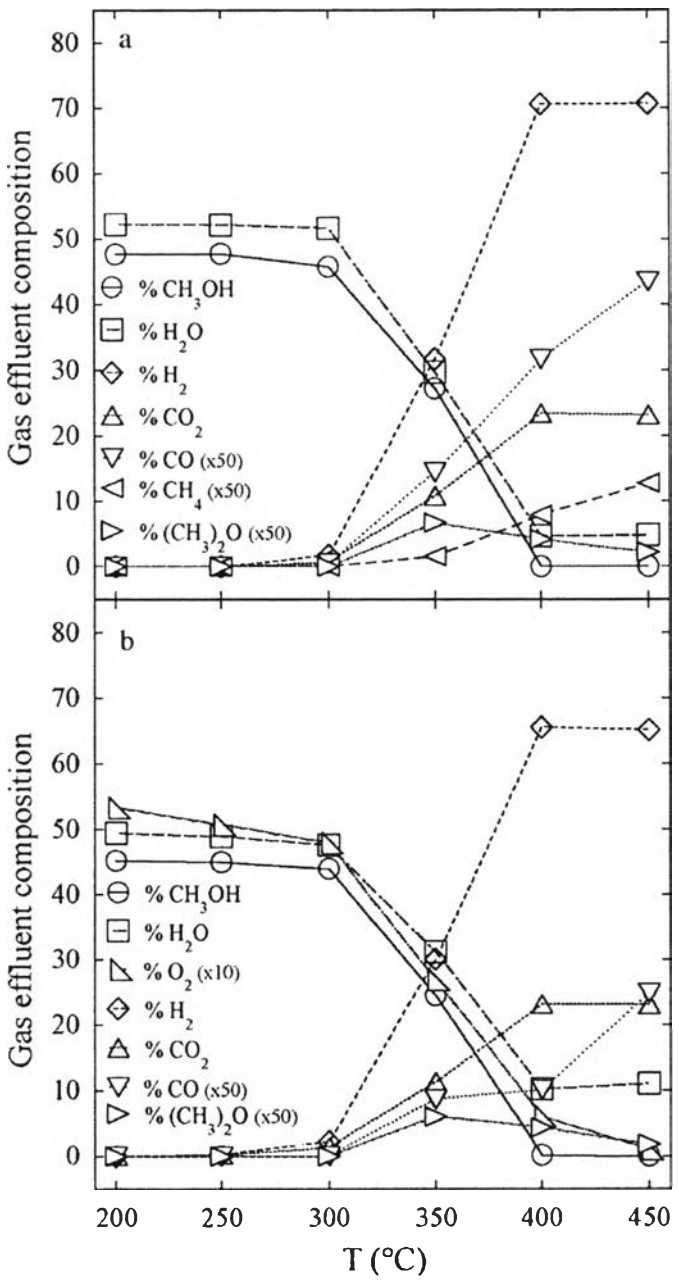

Figure 2.8 Effect of the temperature on the gas effluent composition in the SRM (a) and OSRM (b) reactions over $Zn_{10}Ti_{90}$ (Pinzari *et al.*, 2006).

A comparison between the SRM and OSRM data is shown in Figure 2.8, the hydrogen production of SRM reaction starts at 300°C while the OSRM reaction starts at a lower temperature (250–300 °C), and shows slightly higher methanol conversion than SRM. At temperature of 400 °C, the hydrogen yield of OSRM (2.9a) is higher than the hydrogen yield of SRM (2.9b).

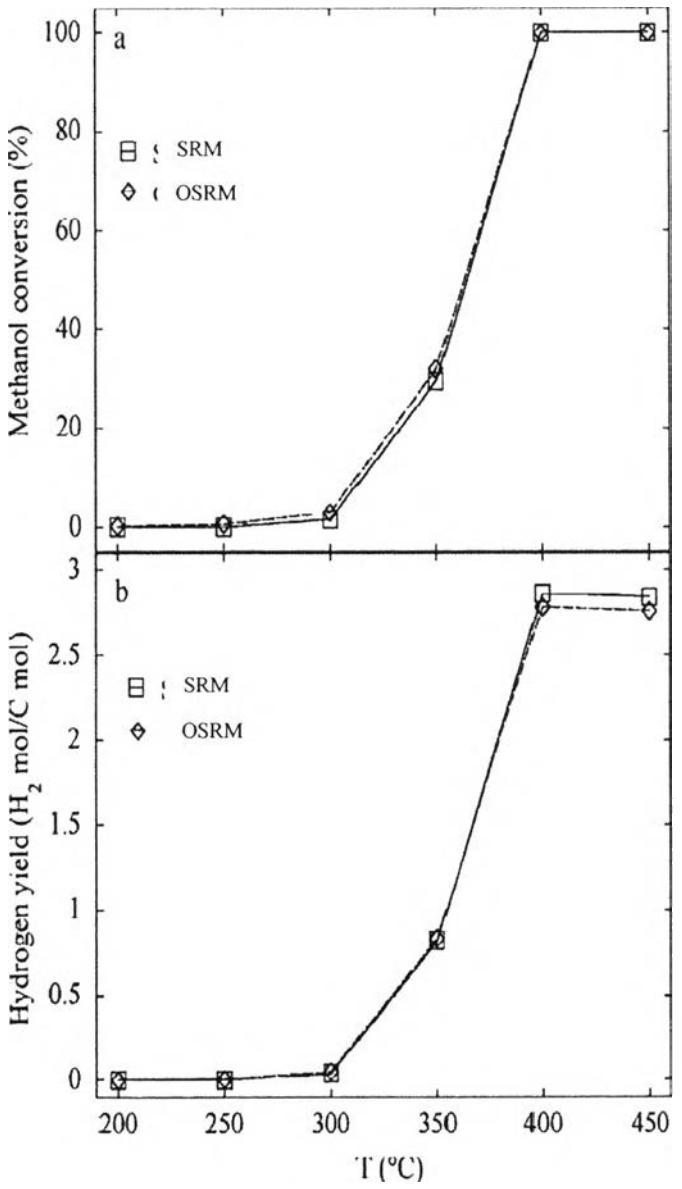

Figure 2.9 Methanol conversion (a) and hydrogen yield (b) as a function of the temperature for $Zn_{10}Ti_{90}$ (Pinzari *et al.*, 2006).

2.2.3.2 Catalytic Activity

The methanol conversion and hydrogen production rate of different catalysts as a function of temperature at various contact-times is displayed in Figure 2.10. The Cu(20)CeAl catalyst exhibited 100% methanol with a hydrogen rate of 179 mmol $s^{-1}kg^{-1}_{cat}$ at 280 °C, which are the highest of methanol conversion, and hydrogen rate. The result showed that methanol conversion increase as a function of temperature for all the catalysts. The enhanced activity of Cu(20)CeAl could be due to higher copper surface area and better copper dispersion.

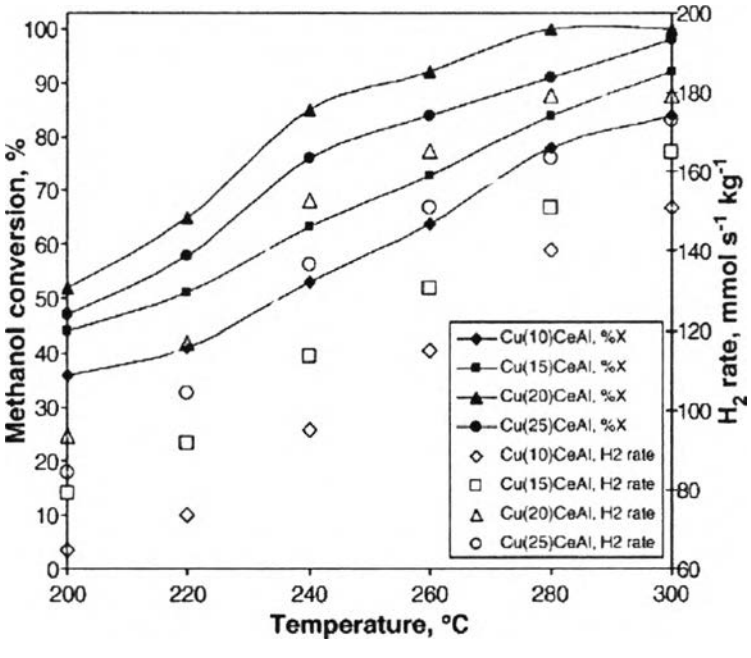

Figure 2.10 Comparison of methanol conversion and hydrogen production rate for different catalysts as a function of temperature. (W/F=15 kg_{cat} s^{-1} $_{molmethanol}$, O/M=0.15 M, S/M=1.5 M, P=1 atm) (Patel *et al.*, 2007).

2.3 Catalysts Development for Steam Reforming and Oxidative Steam Reforming of Methanol

The potential of SRM for hydrogen production in PEM fuel cell applications make researchers try to develop the catalysts for satisfactory performance. The Cu-based catalysts for methanol synthesis are used for the first generation of catalyst.

However, the Cu-based catalysts have many disadvantages such as fast deactivation, and pyrophoric characteristics. Thus, the non-copper catalysts have been investigated for the better performance might be found.

2.3.1 Copper-based Catalysts

Up to now, the widely used catalysts for generating hydrogen from methanol are Cu-based catalysts. The activity of Cu-based catalysts greatly depends on the status of copper, such as copper dispersion, metal surface area, and particle size. However, the rapid deactivation of Cu-based catalyst due to sintering of the metal at temperatures above 300 °C is a barrier to application in OSRM processes (Hong *et al.*, 2008). Cu-containing catalysts are clearly preferred because of their high activity and selectivity at lower temperatures, and Cu-based catalysts supported on or promoted by rare earth are popularly synthesized that improved activity and selectivity. Although Cu catalysts are also regarded as susceptible to thermal deactivation, their sintering abilities may be considerably reduced by the addition of one or more oxide species, such as ZnO, Al_2O_3, or Cr_2O_3 (Mastalir *et al.*, 2005). Moreover, Cu catalysts are still some controversies concerning the nature of active species of Cu. There are some evidences that metallic copper is an active species, and the activity of the catalyst is linearly dependent on the metallic copper surface area of the catalyst. There are many literatures indicating that Cu^+ species helps to increase the activity of the Cu-based catalyst, and it suggests that both Cu^0 and Cu^+ species are essential for hydrogen generation, and the activity of catalyst is dependent on the ratio of Cu^+/Cu^0 in the catalyst. In addition, there are some evidences indicating that Cu^{2+} species is essential for the SRM over Cu/Al_2O_3 catalysts (Wang *et al.*, 2003). The introduction of zinc into Cu/Al_2O_3 catalysts is known to limit the sintering and improving the dispersion of copper. However, Cu/ZnO based catalysts still maintain a primary interest. The role of ZnO as a promoter is explained by the different mechanisms (Maria *et al.*, 2007).

The most interesting catalysts are based on metallic Cu in the presence of Zn, that Zn could increase the dispersion of copper and the stability of Cu^+ species in the catalyst. Figure 2.11 shows the effect of the ratio of Cu/Zn on methanol conversion, and H_2, CO, CO_2 selectivities. It can be seen that the catalyst activity

increases with the increasing of the Cu/Zn ratio and reaches a maximum when the Cu/Zn ratio is 7:3. The results show that the appropriate introduction of Zn is helpful to improve the activity of the catalyst for hydrogen generation.

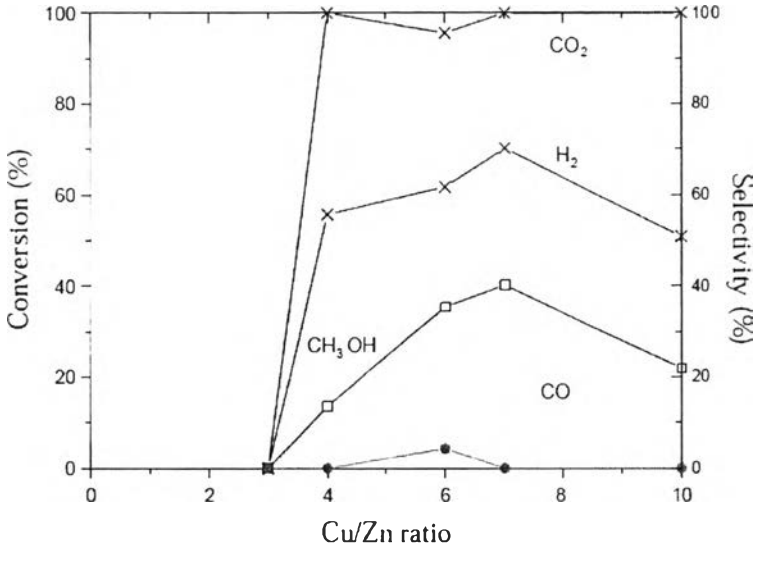

Figure 2.11 Methanol conversion and CO_2, H_2, CO selectivities as functions of Cu/Zn ratios over $Cu/Zn/SiO_2$ catalysts. Reaction conditions: T = 473K; CO_2/CH_3OH = 0:3 (Wang *et al.*, 2003).

It was reported that the Cu catalsyst also depend on the support, the SRM over these Cu/ZrO_2 materials results in substantially reduced CO formation at high methanol conversions compared to the commercial Cu/ZnO catalyst (Ritzkopf *et al.*, 2006). In addition, ZrO_2 was formed to enhance copper dispersion on the catalyst surface of Cu/Zn based catalyst. Among the catalysts tested, $Cu/ZnO/ZrO_2/Al_2O_3$ exhibits the highest methanol conversion, and the lowest CO concentration in the outlet gas that ZrO_2 has an accelerating effect (Jeong *et al.*, 2006).

2.3.2 Non Copper-based Catalysts

Metals from Group 8, 9, and 10, especially palladium (Pd), are highly active in the POM namely, the Pd-based catalysts show a high selectivity at low temperature (Cubeiro *et al.*, 1998). The support of Pd catalyst has an influence on the catalytic performance, the activity of Pd/ZnO for SRM was greatly improved by

previously reducing the catalysts at higher temperatures. The original catalytic functions of metallic Pd were greatly modified as a result of the formation of PdZn alloys. Over the catalysts containing alloys, formaldehyde species formed in the reaction were suggested to be effectively attacked by water, being transformed into CO_2 and H_2 (Iwasa *et al.*, 1995). It was reported that the Pd/ZnO catalysts not only exhibited high activity, but also more importantly very low selectivity to CO for SRM (Chin *et al.*, 2002). The methanol conversion rates were proportional to the H_2 chemisorption uptake, suggesting that the rate determining step was catalyzed by Pd. The study of the interaction between Pd, and ZnO also reported, during reduction of Pd/ZnO catalyst for SRM, the metallic Pd is highly dispersed on ZnO. The strong interaction between Pd and ZnO during the catalyst reduction with hydrogen leads to hydrogen spillover from Pd to ZnO, which causes the reduction of ZnO close to the metallic Pd, and the formation of PdZn alloy. The PdZnAl catalysts were studied for the reactions of WGS, SRM, and RWGS, it was found that the CO selectivities were observed to be lower than the calculated equilibrium values over a range of temperatures, and steam/carbon ratios studied while the reaction rate constants were approximately of the same magnitude for both WGS and SRM. These results indicated that $Pd/ZnO/Al_2O_3$ are active WGS catalysts, WGS is not involved in SRM. RWGS rate constants are in the order of about 20 times lower than SRM, suggesting that RWGS reaction could be one of the sources for small amount of CO formation in SRM (Dagle *et al.*, 2008). However, Pd is an expensive metal and has higher melting point than copper, and is expected to be more resistant to sintering, the stability of PdZn alloy is still an issue, otherwise the Pd is an active catalyst for DCM, which leads to large amount of CO formation (Liu *et al.*, 2006).

2.4 Gold Catalyst

Gold has long been regarded as a poorly active catalyst. Recently, gold catalysts have been attracting rapidly due to their potential applicabilities to many reactions of both industrial and environmental importance. It has atomic number 79 and atomic weight 196.967. The physical properties of Au are shown in Table 2.1

Table 2.1 Physical properties of Au (http://en.wikipedia.org/wiki/Gold)

Phase	Solid
Density	19.3 $g \cdot cm^{-3}$
Liquid density at m.p.	17.31 $g \cdot cm^{-3}$
Melting point	1064.18 °C
Boiling point	2856 °C
Heat of fusion	12.55 $kJ \cdot mol^{-1}$
Heat of vaporization	324 $kJ \cdot mol^{-1}$
Specific heat capacity	25 °C 25.418 $J \cdot mol^{-1} \cdot K^{-1}$

Gold catalysts will be used in commercial applications, including pollution control. The reactions for which gold has already been demonstrated to be a strong catalyst include (Cameron *et al.*, 2003):

- oxidation of CO and hydrocarbons,
- water gas shift (WGS),
- reduction of NO with propene, CO or H_2,
- reactions with halogenated compounds,
- water or H_2O_2 production from H_2 and O_2,
- removal of CO from hydrogen streams,
- hydrochlorination of ethyne,
- selective oxidation, e.g. epoxidation of olefins,
- selective hydrogenation,
- hydrogenation of CO and CO_2.

In addition, gold catalysts have now been demonstrated that heterogeneous gold catalysts are highly active and selective for a number of reactions (water gas-

shift reaction, selective oxidation of CO in hydrogen rich stream, and etc.), often at lower temperatures than existing commercial catalysts. With further technology development, there is clearly the potential to apply catalysis by gold in practical commercial uses, most likely within four broad application areas (Corti *et al.*, 2005):

1. pollution and emission control technologies,
2. chemical processing of a range of bulk and speciality chemicals,
3. the emerging 'hydrogen economy' for clean hydrogen production and fuel cell systems,
4. sensors to detect poisonous or flammable gases or substances in solution.

The gold paricle size has extremely effect to activity of gold catalysts. Nieuwenhuys *et al.* (2002) indicated that nanoparticles gold particles (5 nm) on mixed oxides have been shown to have superior activity for CO oxidation at low temperatures. In low temperature CO oxidation, smaller Au nanoparticles deposited on metal oxides, such as $Mg(OH)_2$, Al_2O_3, TiO_2, and SiO_2, show higher catalytic activity of CO oxidation. However, Haruta *et al.* (2001) studied the deposited Au as nanoparticles on metal oxides by means of co-precipitation and deposition–precipitation techniques. It exhibited surprisingly high catalytic activity for CO oxidation at temperature as low as 200°C. Goodman *et al.* (1998) reported an inspiring result obtained by using a model Au/TiO_2 catalyst. Turn over frequency (TOF) for CO oxidation reaches a maximum at a diameter of Au islands of 3.5 nm (3 atoms thick) where Au partially loses its metallic nature, as shown in Figure 2.12. They suggested that this transition might be correlated to the high catalytic activity. Since the sample used for catalytic activity measurements was composed of the Au islands with a certain size distribution. They summarized that the catalytic activity in CO oxidation over Au/TiO_2 model catalyst was dependent on the Au cluster size with a maximum occurring at about 2–3 nm.

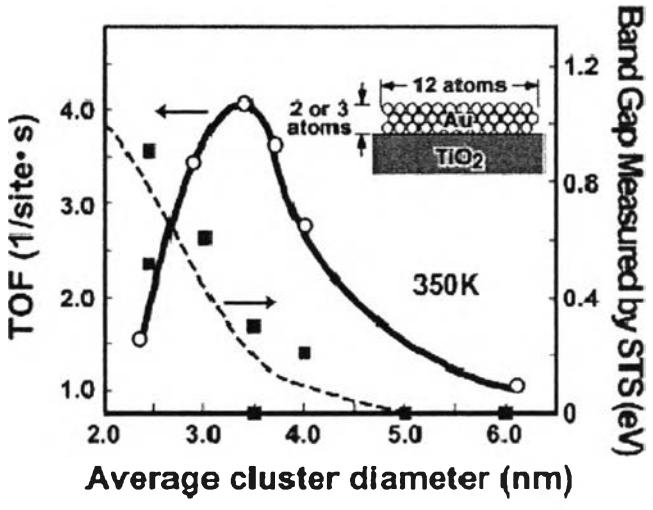

Figure 2.12 Turn over frequencies and band-gap measure by STM as a function of the diameter of Au islands deposited on TiO_2 (Goodman *et al.*, 1998).

2.5 Supported Catalyst

Ceria (CeO_2) support is known as a very attractive support material, for improvement the stability of catalysts due to its ability to maintain a high dispersion of the active components and to change its oxidation state of the cation between Ce^{3+} and Ce^{4+} (redox condition) as an active site (Tabakova *et al.*, 2011). Henderson *et al.* (2002) purposed that over defect oxide surfaces were the active sites of water dissociation. During hydrogen prereduction in this study, ceria is highly reduced and more oxygen anion vacancies are created on the ceria surface. CeO_2 is such a strong reducing reagent that it can decompose water into hydrogen; therefore, water can be activated by the reduced ceria. It is noted that the production of CO_2 consumes one surface oxygen. Figure 2.13 involves with four distinct steps: (i) the adsorption of methanol and water at the Cu/CeO_2 interface, (ii) the surface reaction and the desorption of gaseous products, (iii) the migration of surface oxygen from CeO_2 to the reduced Cu (oxygen reverse spillover), (iv) the regeneration of partially oxidized copper and oxygen vacancies.

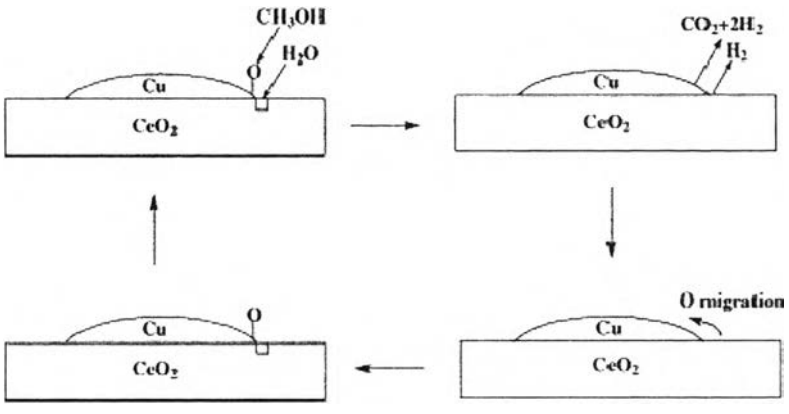

Figure 2.13 Proposed reaction mechanism for SRM at the Cu/Ce interface (Men *et al.*, 2004).

It showed that ceria plays the role of an active support capable of producing oxygen. The high and stable activity of Au/CeO_2 catalysts could arise from the high and stable gold dispersion present during the catalytic operation (Andreeva *et al.*, 2002). The Au/CeO_2 catalysts prepared by the deposition–precipitation method was the most active catalyst at temperatures between 100 and 250 °C without producing methane below 623 °C. It was reported that the WGS reaction proceeds over the perimeter interfaces of small gold particles on a reduced cerium oxide surface (Sakurai *et al.*, 2005). In addition, they studied the methanol steam reforming over Au/CeO_2 catalyst, and the effect of catalyst preparation: Incipient Wetness Impregnation (IWI), Co-precipitation (CP), and Deposition-precipitation (DP) on the catalytic activities. The results showed that the DP exhibited the smallest gold particle size and the highest methanol conversion. Moreover, the activity of gold catalyst supported on various oxides in CO oxidation reaction and their improvement by inclusion of an iron component. They found that addition of iron in the preparation lowered the rate of deactivation when TiO_2, SnO_2, and CeO_2 were used as supports (Mareau *et al.* 2006).

For another interesting support, iron oxide (Fe_2O_3) is also an attractive support due to an interaction between Au and Fe_2O_3 could lead to the formation of an

active phase at the interface of the catalyst. The proposed the schematic model of oxidation of CO oxidation on the prepared Au/Fe_2O_3 is shown in Figure 2.14. All of explanations in each step are shown as follows:

1. adsorption of CO onto hydrated Au particle,
2. formation of hydroxycarbonyl, spillover to Au–support interface (i), and oxidation to bicarbonate by lattice oxygen (ii),
3. decomposition of the bicarbonate to produce CO_2 and H_2O,
4. further CO adsorption on Au particle and O_2 adsorption in oxygen vacancy of the Fe_2O_3,
5. H_2O attack of carbonate at interface for further bicarbonate formation (6).
6. decomposition of bicarbonate yields CO_2, and recycles OH to continue the catalytic cycle (8),
7. (9) shows reaction of bicarbonate with OH to form H_2O and stable carbonate at interface.

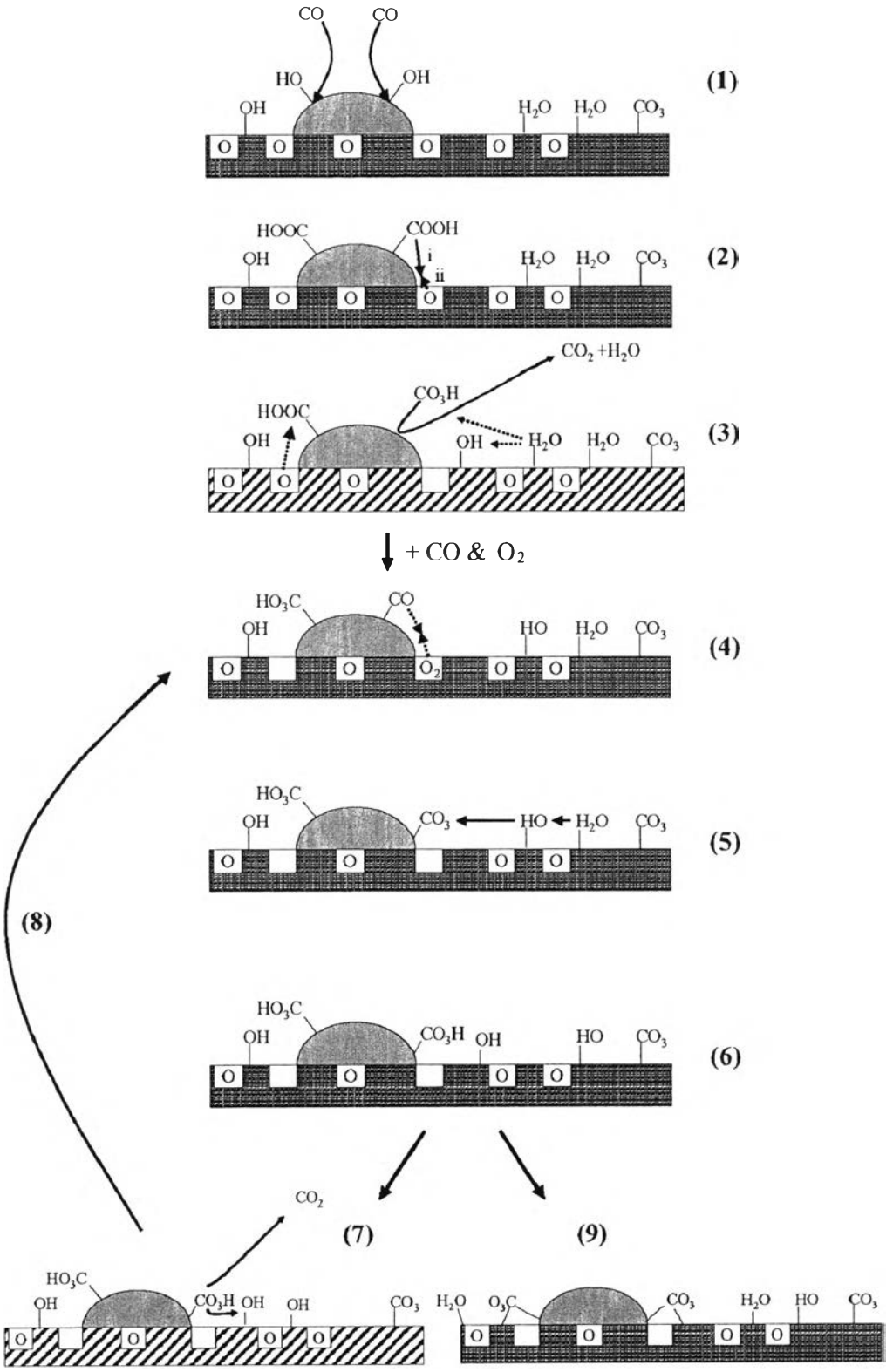

Figure 2.14 Schematic model of oxidation of CO on as prepared (dried) Au/Fe_2O_3 (Makkee *et al.*, 2005).

In addition, oxide ions inside the lattice are also removable, and a whole of nonstoichiometric oxides between CeO_2 and Ce_2O_3. It is well known that the lattice oxygen mobility and concomitant oxide ion conductivity in cerium oxide can be increased by the substitution of another metal ion for cerium. Because the ceria shows much improved properties under doping, a lot of ceria-based systems have been investigated. It has been proved that the lower valence ions in ceria influence the energetic properties by lowering the activation energy for oxygen migration (Vidmar *et al.*, 1997). The catalytic activity for methane selective oxidation by using $Ce_{1-x}Fe_xO_2$ complex oxides was also studied. The characteristic results revealed that the combination of Ce and Fe oxide in the catalysts could lower the temperature necessary to reduce the cerium oxide. The catalytic activity for selective CH_4 oxidation was strongly influenced by dropped Fe species. Adding the appropriate amount of Fe_2O_3 to CeO_2 could promote the action between CH_4 and CeO_2 (Kongzhai *et al.*, 2008).

Hongyan *et al.* (2008) studied the catalytic properties for ethanol steam reforming by using $Ce_xFe_{1-x}O_2$ solid solution catalyst. Figure 2.15 (a) shows the XRD patterns of the $Ce_xFe_{1-x}O_2$ solid solutions. The $Ce_xFe_{1-x}O_2$ solid solution had a higher surface area than the pure Fe and Ce oxides. The addition of a small amount of Fe into CeO_2 resulted in a remarkable increase in the surface area. Raman spectra (Figure 2.15 (b)), confirmed that part of the Ce^{4+} cations in CeO_2 were substituted by Fe^{3+} cations, which resulted in the formation of a $Ce_xFe_{1-x}O_2$ solid solution. From Figure 2.16, it is clear that the $Ce0.90Fe0.10O_2$ catalyst showed higher ethanol conversion and hydrogen concentration than the CeO_2 and α-Fe_2O_3 catalysts.

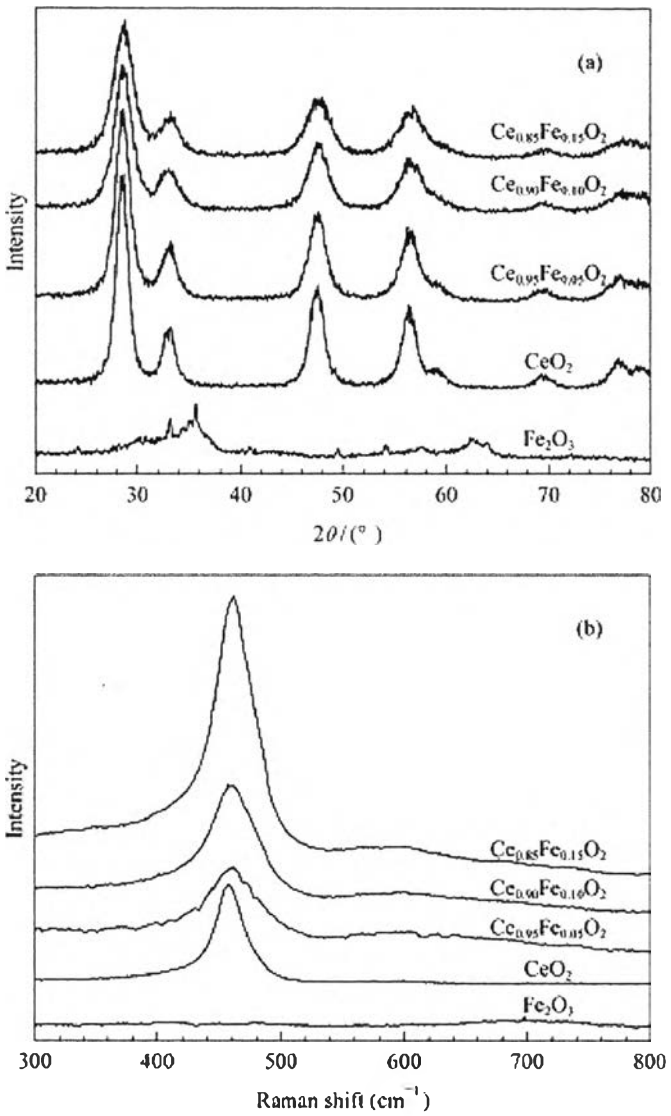

Figure 2.15 XRD patterns (a) and Raman spectra (b) of different samples of composited oxide catalysts (Hongyan *et al.*, 2008).

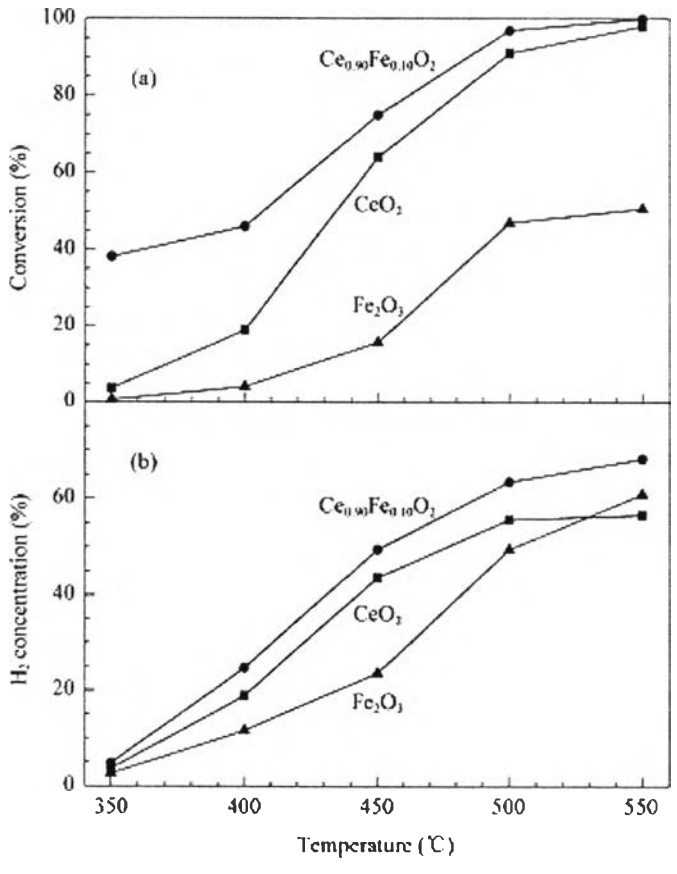

Figure 2.16 Ethanol conversion (a) and hydrogen concentration (b) in the effluent of steam reforming of ethanol as a function of reation temperature over different samples (Hongyan *et al.*, 2008).

The comparison of the catalytic performance in terms of CO conversion, and selectivity of the catalysts versus reaction temperature, is shown in Figure 2.16. Au/CeO_2 and Au/Ce50Fe50 catalysts showed high CO oxidation activity at room temperature. Au/Ce50Fe50 catalysts demonstrated the best catalytic behavior in the operation temperature range of PEM fuel cell. Its activity increased with increasing temperature, and reached 98.5% (with 42% selectivity) at 70 °C. In addition, when CO_2 and H_2O were simultaneously present in the feed. Au/Ce50Fe50 was found to be the most resistant toward deactivation by CO_2 and water.

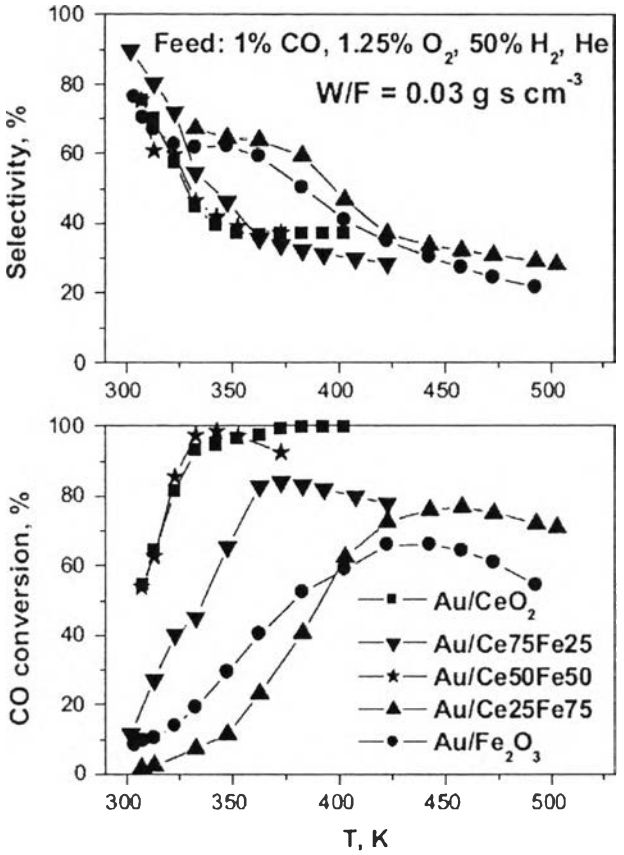

Figure 2.17 Activity and selectivity towards CO_2 production of Au/CeO_2 (■), Au/Ce75Fe25 (▼), Au/Ce50Fe50 (▯), Au/Ce25Fe75 (▲), and Au/Fe_2O_3 (●) catalysts for the PROX reaction at W/F=0.03gscm^{-3}. Feed: 1% CO, 1.25% O_2, 50% H_2, He. (Tabakova *et al.*, 2011).

All of these are the motivation in this work to study effect of composite support (CeO_2–Fe_2O_3), Au content, steam-methanol molar ratio, oxygen-methanol molar ratio, and reaction temperature on the catalytic activity for the OSRM. In particular, the physical and electronic properties of a gold catalyst are greatly affacted by using CeO_2–Fe_2O_3 as support.